Absence of Thyroid Hormone Activation during Development Underlies a Permanent Defect in Adaptive Thermogenesis

Jessica A. Hall,* Scott Ribich,* Marcelo A. Christoffolete, Gordana Simovic, Mayrin Correa-Medina, Mary Elizabeth Patti, and Antonio C. Bianco

Biological and Biomedical Sciences Program (J.A.H., A.C.B.), Division of Endocrinology, Diabetes, and Hypertension, Brigham and Women's Hospital (S.R., M.A.C.), and Research Division, Joslin Diabetes Center (M.E.P.), Harvard Medical School, Boston, Massachusetts 02115; and Division of Endocrinology, Diabetes, and Metabolism (G.S., M.C.-M., A.C.B.), University of Miami Miller School of Medicine, Miami, Florida 33136

Type 2 deiodinase (D2), which is highly expressed in brown adipose tissue (BAT), is an enzyme that amplifies thyroid hormone signaling in individual cells. Mice with inactivation of the D2 pathway (D2KO) exhibit dramatically impaired thermogenesis in BAT, leading to hypothermia during cold exposure and a greater susceptibility to diet-induced obesity. This was interpreted as a result of defective acute activation of BAT D2. Here we report that the adult D2KO BAT has a permanent thermogenic defect that stems from impaired embryonic BAT development. D2KO embryos have normal serum T3 but due to lack of D2-generated T3 in BAT, this tissue exhibits decreased expression of genes defining BAT identity [*i.e. UCP1*, *PGC-1*α and *Dio2* (nonfunctional)], which results in impaired differentiation and oxidative capacity. Coinciding with a reduction of these T3-responsive genes, there is oxidative stress that in a cell model of brown adipogenesis can be linked to decreased insulin signaling and decreased adipogenesis. This discovery highlights the importance of deiodinase-controlled thyroid hormone signaling in BAT development, where it has important metabolic repercussions for energy homeostasis in adulthood. **(*Endocrinology* 151: 4573–4582, 2010)**

Brown adipose tissue (BAT) is a major site of adaptive thermogenesis, having gained recent appreciation for presence and activity in adult humans (1). Its capacity to convert chemical energy into heat is used to preserve thermal and caloric homeostasis. Both pathways rely on uncoupling protein 1 (UCP1), a thyroid hormone-responsive gene (2). While small mammals use BAT activation to defend core temperature in the cold, hypothyroid animals succumb within hours because of insufficient BAT thermogenesis (3, 4).

Thyroid hormone signaling can be controlled in individual cells through the selective activation or inactivation of thyroid hormone via the deiodinases (5). Although thyroid hormone primarily exists as the minimally active prohormone T4 (thyroxine), extrathyroidal tissues can convert T4 to the biologically active T3 (3,5,3′-tri-iodothyronine), which binds thyroid hormone receptor (TR) to regulate transcription of T3-responsive genes. This reaction is catalyzed by the type 2 deiodinase (D2), while both T4 and T3 can be inactivated by the type 3 deiodinase (D3) (Fig. 1, A and B, respectively). As a result, D2-expressing cells have a higher T3 concentration and TR activation. Correspondingly, D3-expressing cells can inactivate incoming T3, thereby reducing TR activation, such as during myocardium hypoxia (6).

While the serum concentration of T3 is normal in mice with targeted deletion of D2 gene (D2KO) (7), BAT thermogenesis is severely impaired (8). Freshly isolated D2KO brown adipocytes have impaired lipogenesis, generate less cAMP, and fail to increase metabolic rate in response to

ISSN Print 0013-7227 ISSN Online 1945-7170
Printed in U.S.A.

doi: 10.1210/en.2010-0511 Received May 6, 2010. Accepted June 10, 2010.
First Published Online July 21, 2010
* J.A.H. and S.R. contributed equally to this study.

For editorial see page 4087

Abbreviations: BAT, Brown adipose tissue; *C/EBP*α, CCAAT/enhancer-binding protein-α; D2, type 2 deiodinase; D2KO, *Dio2* gene knockout; DTT, dithiothreitol; iBAT, interscapular brown adipose tissue; *PPAR*γ, peroxisome proliferator-activated receptor-γ; ROS, reactive oxygen species; T3, 3,5,3′-tri-iodothyronine; T4, thyroxine; TR, thyroid hormone receptor; UCP1, uncoupling protein 1; UPLC, Ultra Performance Liquid Chromatography; WT, wild type.

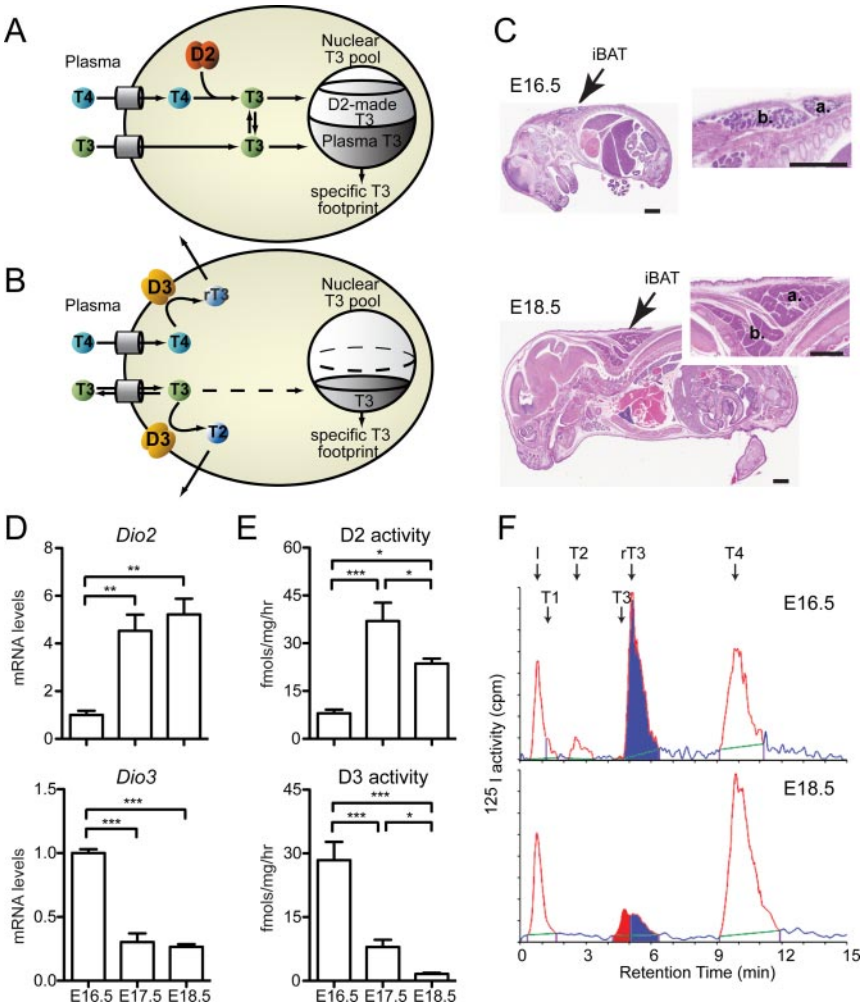

FIG. 1. Deiodinase expression during BAT development. A and B, Schematic of D2 and D3 modulation of thyroid hormone signal. D2 converts T4 to T3 (A), increasing nuclear T3 levels, while D3 can inactivate T3 and T4 (B), decreasing thyroid hormone signal. C, Image of H&E section of wild-type mouse embryo at E16.5 (*top*) and E18.5 (*bottom*) with arrow indicating interscapular BAT (iBAT). *Inset* shows enlarged iBAT, where a. is section of BAT dissected for subsequent analyses. *Bars*, 1 mm. D, *Dio2* and *Dio3* mRNA levels of embryonic BAT graphed relative to E16.5 expression. E, D2 and D3 activity of BAT sonicates from E16.5, E17.5, and E18.5 embryos. *, $P < 0.05$; **, $P < 0.01$; and ***, $P < 0.001$ by one-way ANOVA with Newman-Keuls Multiple comparison. F, Chromatogram of T4-fate, as resolved by UPLC, when E16.5 (*top*) and E18.5 (*bottom*) BAT sonicates are incubated with ^{125}I-T4. Deiodination products are labeled by arrow according to retention time. Area depicting T3 peak is colored in *red*; rT3 peak in *blue*.

adrenergic stimulation (8, 9). D2KO animals can only survive in the cold due to an increase in BAT sympathetic activity and shivering, a behavior not normally observed in cold-exposed mice. In addition, D2KO mice are more susceptible to obesity when placed on a high-fat diet (Castillo & Hall *et al.*, unpublished).

Here we investigated whether insufficient D2KO BAT thermogenesis stems from impaired BAT development or results primarily from defective activation of the mature tissue. We have found that absence of D2-mediated thyroid hormone signaling in embryonic BAT contributes to a decrease of T3-responsive genes, such as *PGC-1α*, *UCP1*, and *Dio2*. Furthermore, in D2KO embryonic BAT there is oxidative stress, which in a cell model of brown adipogenesis can lead to decreased insulin signaling and impaired differentiation. These data illustrate the critical role played by D2 in BAT development, the absence of which results in a defective mature brown adipocyte.

Materials and Methods

Materials

Unless otherwise specified, reagents were purchased from Sigma-Aldrich (St. Louis, MO). BODIPY 493/503, Fungizone, Trizol, Oil Red O, and SlowFade Gold with DAPI were from Invitrogen (Carlsbad, CA). Anion exchange resin AG1-X8 was obtained from Bio-Rad (Richmond, CA). Anti-Phospho-Akt (Ser473), anti-Akt, anti-Phospho-IRS-1 (Ser307), and anti-Phospho-IκBα (Ser32) antibodies were obtained from Cell Signaling (Danvers, MA). The antirabbit Alexa647, antirabbit Alexa488, and antirabbit Alexa593 antibodies were from Invitrogen. Outer-ring labeled ^{125}I-T4 and -T3 were purchased from PerkinElmer (Boston, MA) and purified on LH-20 columns (Sigma) before use. Dithiothreitol (DTT) was from Calbiochem (San Diego, CA).

Animals

All studies were performed according to protocols approved by the Animal Care and Use Committees of Harvard Medical School and University of Miami Miller School of Medicine. Mice with targeted disruption of the *Dio2* gene (D2KO) were backcrossed into a C57BL/6J background for 10 generations. Genotyping of D2KO mice was as previously described (9). C57BL/6J mice (wild-type, WT) were purchased from Jackson Laboratories (Bar Harbor, MA). For the embryo studies, WT mice were mated with D2KO mice to generate mice heterozygous for the D2KO allele (D2Het mice). Timed-pregnant dams of D2Het pairs were used to obtain littermate embryos of WT, D2Het and D2KO genotypes. Pregnancy was determined by presence of a vaginal plug (embryonic d 0.5, E0.5). All mice were maintained on normal chow and housed under a 12-h light, 12-h dark cycle at 22 C.

Histology

Hematoxylin and eosin staining was performed on paraffin-embedded sections of embryos that had been fixed in 10% neutral buffered formalin.

Deiodination assays

D2 and D3 activity was determined as previously described (10). D2 activity was measured on 30–40 μg protein of BAT

homogenates in the presence of outer-ring labeled ^{125}I-T4, 0.1 nM T4 substrate, and 20 mM DTT for 4 h at 37 C and ^{125}I release quantified with a γ counter (2470 WIZARD^2, PerkinElmer Life Sciences, Boston, MA). Samples treated with 100 nM T4 (saturating) were used for background measurements. D3 activity was assayed by quantification of deiodination products on UPLC (ACQUITY, Waters Corporation, Milford, MA) after 1-h incubation at 37 C with outer-ring labeled ^{125}I-T3, 0.1 nM T3 substrate, 1 mM PTU, and 10 mM DTT. For determination of T4-fate, deiodination products were resolved by Ultra Performance Liquid Chromatography (UPLC) after incubation for 2 h with outer-ring labeled ^{125}I-T4, 1 mM PTU, and 10 mM DTT.

Plasma hormone levels

Plasma levels of TSH, T4, and T3 were determined using a MILLIPLEX rat thyroid hormone panel kit as described by the manufacturer (Millipore, Billerica, MA) and read on a BioPlex (Bio-Rad, Hercules, CA). Plasma from hypo- and hyperthyroid mice (treated for 10 d with Sodium Perchlorate and Methimazole or 80 mg/kg T4, respectively) was used to prepare mouse TSH standards. Both rat and mouse curves were parallel and separated by a factor of 5. Mouse embryo serum samples were diluted 1:2.5 for analysis, and settings for the BioPlex included a modified specification of 100 events per bead.

Brown preadipocyte tissue culture

Interscapular brown adipose tissue (iBAT) was dissected from male and female mice from 4–8 wk of age and processed as previously described (11). Unless indicated, cells were grown in DMEM + 10% fetal bovine serum, supplemented with 10 mM HEPES, 10^{-7} M sodium selenite, 3 nM insulin, 25 mg/liter tetracycline, 25 mg/liter streptomycin, 25 mg/liter ampicillin, and 1 mg/liter fungizone. The preadipocytes were propagated and plated at confluence (20,000 cells/cm^2), corresponding to d 0 of differentiation. Cells were differentiated for 10 d in this media unless noted. T3-responsiveness was performed with thyroid hormone-depleted serum (AG1-X8 resin/charcoal-stripped) as previously described (11). An adipogenic cocktail of indomethacin (125 μM), IBMX (0.5 mM), and dexamethasone (0.5 μM) was used with or without insulin in indicated experiments. Other treatments included Ascorbic Acid (1 mM), rT3 (200 nM), and T3 (50 nM or 100 nM).

Microscopy and cell counting

For the cell counting experiments, d 0 cultures were differentiated on LabTek permanox slides (Nalge Nunc International, Rochester, NY). Cells were fixed in 4% PFA, and immunocytochemistry performed as suggested by antibody manufacturers (Abcam and Invitrogen). Slides were imaged on a Nikon Eclipse 90i microscope (Melville, NY), with a total of 15 fields in three different wells acquired for each sample at each time point. The location of individual fields was kept consistent between slides with a reference guide on the microscope stage. Nuclei or cells were counted using the Nikon NIS-Elements imaging software (for DAPI), or manually (for BODIPY 493/503). Identical thresholds for fluorescent intensity were used for WT and D2KO fields. Percent differentiation was determined as fraction of cells staining for BODIPY 493/503.

Cellular O_2 consumption

Ten-day differentiated WT and D2KO brown adipocyte cultures were seeded in 24-well microplates and assayed in the XF24 instrument from Seahorse Bioscience (Billerica, MA), as described previously (12).

Quantitative RT-PCR

For expression analyses of embryonic BAT, total RNA was extracted using RNeasy Lipid Tissue Mini kit (Qiagen Sciences) and contaminating DNA removed with TURBO DNA-free (Ambion), followed by cDNA preparation from 0.3–1 μg of total RNA with Applied Biosystem's High Capacity cDNA RT kit. For cell culture samples, total RNA was extracted using the Trizol method, and 1.5–10 μg of total RNA was used in the SuperScript First-Strand Synthesis System for RT-PCR (Invitrogen) on a Robocycler (Stratagene, La Rolla, CA). For mitochondrial DNA content, DNA was recovered during the Trizol RNA isolation, and 18 ng of total DNA used for amplification. cDNA products were quantified by real-time PCR using the SYBR Green FastMix (Quanta) on a MyiQ iCycler (Bio-Rad) under conditions as previously described (9). Primer sequences available upon request. Gene expression was determined by generation of a standard curve and normalized for the expression of *Cyclophilin B*.

Insulin signaling and Western blotting

For insulin signaling experiments, brown preadipocyte cultures were serum starved for 20 h. Cells were stimulated with varying insulin concentrations (0–7.5 nM) for 5 min, and then lysed in 50 mM HEPES (pH 7.4), 137 mM NaCl, 1 mM $MgCl_2$, 1 mM $CaCl_2$, 10 mM sodium pyrophosphate, 10 mM NaF, 2 mM EGTA, 2 mM Na_3VO_4, 2 mM phenylmethylsulfonylfluoride, 1% NP-40, and 10% Glycerol. Extracts were sonicated, total lysates separated on a pre-cast gel (Bio-Rad), transferred to Immobilon-P transfer membranes (Millipore, Bedford, MA), and blotted as directed by manufacturer. Western blots were stripped using Restore PLUS Western Blot Stripping Buffer (Thermo Scientific, Rockford, IL) as directed. Scanned images were processed in Adobe Photoshop Elements 2.0 software and auto levels used to increase brightness for publication.

Reactive oxygen species (ROS) detection by flow cytometry

WT and D2KO preadipocyte cultures were pretreated for 30 min with 5 mm CM-H_2DCFDA (Invitrogen) and subsequently harvested and washed with PBS. Cell suspensions were immediately sorted at the Dana-Farber Cancer Institute Flow Cytometry Core Facility (Boston, MA) Core. Data analysis was performed with the FlowJo Flow Cytometry Analysis Software (Ashland, OR), with a lower cutoff of 1000 FL intensity for the CM-H_2DCFDA dye.

Detection of lipid peroxidation

Embryonic BAT was frozen in liquid nitrogen upon dissection and stored at −80 C until analysis. For homogenization, tissue was resuspended in cell lysis buffer (Cell Signaling) containing a complete protease inhibitor cocktail from Roche (Basel, Switzerland) and sonicated. Protein concentration was determined using the Bradford method (Bio-Rad). Lipid peroxidation was detected on 20 μg of BAT protein lysate with the OxiSelect Malondialdehyde (MDA) Immunoblot kit (Cell Biolabs) using a rabbit anti-MDA antibody according to the manufacturer's instructions.

Statistical analysis

Data were analyzed using PRISM software (GraphPad Software, Inc, San Diego, CA) and expressed as mean ± SEM. Western blot signal was analyzed with ImageJ software (National Institutes of Health, Bethesda, MD) and normalized to α-tubulin signal on each blot. A two-tailed Student's *t* test or one-way ANOVA with Newman-Keuls Multiple Comparison test (or Dunnett's Multiple Comparison test, where indicated) was used to compare means between groups.

Supplemental experimental procedures

For details on experiments included in Supplemental Data, please refer to the Supplemental Experimental Procedures published on The Endocrine Society's Journals Online web site at http://endo.endojournals.org.

Results

Local thyroid hormone signaling increases during brown adipogenesis

It is not known whether D2 plays its critical role during development of BAT or exclusively during acute activation of mature BAT. To address this question, we focused on BAT development during embryonic life, where embryos are held *in utero* at thermoneutrality, allowing for capture of D2-mediated events of an adipogenic nature. In rodents, BAT develops late during the prenatal period, such that at birth the BAT is equipped with its full thermogenic potential (13). Using a mouse model of BAT development, an interscapular BAT depot became evident at embryonic d (E)16.5, reaching a substantial size by E18.5 (~5 mm) (Fig. 1C). With this 3-d developmental snapshot to study *in vivo* adipogenesis, we then analyzed the mRNA transcripts of D2 and D3 (*Dio2* and *Dio3*, respectively). *Dio2* expression increased considerably from E16.5 to E18.5, reaching levels over 5-fold greater by E18.5 (Fig. 1D). This corresponded with a decrease in *Dio3*, from its highest expression level at E16.5 to 27% by E18.5. Deiodinase activity correlated with mRNA levels for D3, where its highest activity was observed at E16.5. On the other hand, D2 activity increased from E16.5 to E18.5, with peak D2 activity at E17.5 (Fig. 1E).

We verified that these reciprocal changes in deiodinase activity modify thyroid hormone signaling in the developing brown adipocyte by following the fate of the prohormone T4 during incubation with E16.5 or E18.5 BAT sonicates (Fig. 1F). At E16.5, almost all T4 exposed to BAT sonicates was inactivated to rT3 (via D3), and no T3 was detected, as it was rapidly inactivated to T2 (via D3). This indicates that early during brown adipogenesis thyroid hormone signaling is kept at a minimum as both T4 and T3 are inactivated by high levels of D3. On the other hand, at E18.5, there was an identifiable peak of T3, resulting from T4 activation by D2. At the same time, rT3 production decreased dramatically, and T3 inactivation to T2 was undetected. Thus, coordinated changes in deiodinase behavior mediate an increase in thyroid hormone signaling during BAT development. These patterns of deiodinase expression were also found by comparing *in vitro* proliferating brown preadipocytes with isolated mature brown adipocytes (Supplemental Fig. 1).

Impaired expression of T3-dependent genes disrupts D2KO brown adipogenesis

To test the hypothesis that D2-generated T3 plays a role during BAT development, we studied D2KO embryos from E16.5-E18.5. By breeding mice heterozygous for the D2KO allele (D2Het), we could compare D2KO and D2Het embryos with WT littermates. Importantly, we determined that E18.5 D2KO and D2Het embryos are systemically euthyroid with normal concentrations of T3 in plasma (Fig. 2A), which is a phenotype that persists into adulthood (7). This is further supported by an analysis of 81 E18.5 WT, D2Het, and D2KO embryos, which had similar body weight and length (Supplemental Table 1). Thus, differences between WT and D2KO BAT should reflect effects based on a local (tissue-specific) decrease in thyroid hormone signaling.

Although we were unable to find gross differences in BAT pad appearance or size between E18.5 WT and D2KO littermates (data not shown), we sought to detect changes at the transcript level that would shed light on BAT integrity. First, we looked at the expression of genes common to both white and brown adipogenesis, including the antiadipogenic preadipocyte factor-1 (*Pref1*; also known as *DLK1*) and *Dio3* (both genes are in the same locus) (14–16), and the master transcriptional regulators of adipogenesis CCAAT/enhancer-binding protein-α (*C/EBPα*) and peroxisome proliferator-activated receptor-γ (*PPARγ*) (17). Notably, while there was a trend for lower expression of *PPARγ2* in the D2KO BAT, the expression of the terminal differentiation marker, *aP2*, which is a target of *PPARγ*, was significantly decreased by E18.5 in D2KO BAT (25% lower than WT) (Fig. 2B). Second, we looked at genes selective for the molecular signature of brown adipocytes, where we found *Cidea,* which can modulate UCP1 activity (18), to be reduced 20% in D2KO E18.5 BAT, but other genes preferentially expressed in brown *vs.* white adipocytes (*PRDM16*, *Elovl3*, *PPARα* and *Cox8b*) to be unaffected (Fig. 2C). Third, we examined the expression of several genes important for the thermogenic function of BAT. *UCP1* increased dramatically during the course of development, but 54% of this induction was lost by E18.5 in D2KO BAT (Fig. 2D). D2KO mice still express a nonfunctional mRNA of *Dio2* (7), and

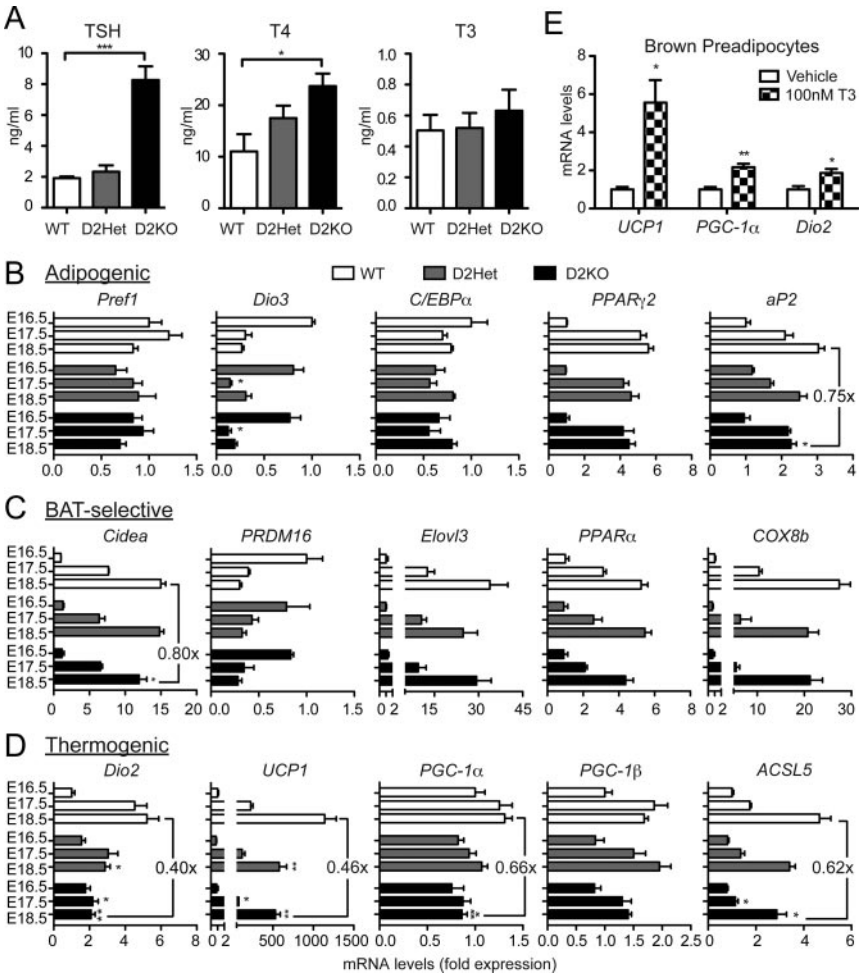

FIG. 2. D2-generated T3 contributes to brown fat identity. A, Plasma TSH, T4, and T3 concentrations of E18.5 WT (n = 3), D2Het (n = 8), and D2KO (n = 5) E18.5 embryos from 5 litters. B–D, Expression of selective genes in iBAT from WT, D2Het, and D2KO embryos at embryonic d E16.5, E17.5, and E18.5. mRNA levels were determined by qRT-PCR and are graphed relative to E16.5 WT expression. Genes are grouped into (B) genes common to both white and brown adipogenesis, (C) genes that are specific to BAT, and (D) genes that are involved in thermogenesis. *, $P < 0.05$; **, $P < 0.01$; and ***, $P < 0.001$ *vs.* WT of respective day by one way ANOVA with Dunnett's Multiple Comparison test. E, Gene expression in confluent brown preadipocytes after 24 h in stripped serum plus vehicle or 100 nM T3. *, $P < 0.05$; and **, $P < 0.01$ by Student's *t* test.

without D2 activity, the developmental induction of *Dio2* and *PGC-1α* were also significantly blunted (60% and 34% decreased, respectively). *PGC-1β* was slightly decreased in late prenatal D2KO BAT, but this difference did not reach statistical significance. Long-chain acyl-CoA synthetase (*ACSL5*), which plays a role in β-oxidation, was also significantly decreased in D2KO E18.5 BAT (38%). Moreover, BAT from D2Het embryos tended to have an intermediate phenotype, at times behaving more like WT BAT (*i.e.* expression of *Cidea*), and at other times like D2KO BAT (*i.e.* expression of *UCP1*), suggesting that BAT impairment is related to dose of the *Dio2* gene. In fact, whereas embryonic D2KO BAT has no D2 activity, heterozygotes have ~50% less D2 activity in BAT compared with WT (data not shown).

Thus, targeted disruption of *Dio2* selectively impairs the expression of key molecules in brown adipogenesis involved in fatty acid metabolism (aP2, Cidea, and ACSL5) and mitochondrial respiration (UCP1, PGC-1α and D2). To test the hypothesis that these are T3-responsive pathways, we turned to an *in vitro* primary culture model of differentiating brown preadipocytes, in which differentiation is induced in 10 d driven only by low levels (3 nM) of insulin (Supplemental Fig. 2, A–C). These cells are propagated in 10% fetal bovine serum, which provides physiological levels of thyroid hormone (19). In this setting, induction of *aP2*, *Cidea*, *UCP1*, and *PGC-1α* in D2KO brown adipocytes were progressively less than WT cultures (Supplemental Fig. 2D and data not shown). Additionally, *C/EBPα* and *PPARγ2* reached levels lower than 50% of WT by d 10. An expanded search of several downstream targets of *C/EBPα* and *PPARγ2* led to the detection of 13 additional genes with known roles in brown adipocyte function that were insufficiently induced in D2KO cells (Supplemental Fig. 2D). Lastly, gene responsiveness to T3 was tested in confluent WT brown preadipocytes exposed to T3 for 24 h, which resulted in a 5.5-fold induction of *UCP1*, and about 2-fold induction of *PGC-1α* and *Dio2*, confirming direct responsiveness to T3 (Fig. 2E). On the other hand, prolonged T3 exposure (6 d) caused the additional stimulation of *PPARγ2* and *CEBPα* (data not shown). Taken together, these data indicate a role for D2-generated T3 in BAT development, where the enhanced thyroid hormone signaling provided by intracellular T3 production primes the mature tissue with molecular aspects required for adaptive thermogenesis.

Confirming that these reductions in the expression of T3-responsive genes were detrimentally affecting the differentiation process, the phenotype of the D2KO cells included a delay in the maturation process as assessed by lipid accumulation via immunofluorescence after staining with the lipid-specific dye BODIPY 493/503 (Fig. 3A). D2KO adipocyte cultures contained a lower fractional number of lipid-containing cells (37% lower at d 10), indicating that fewer

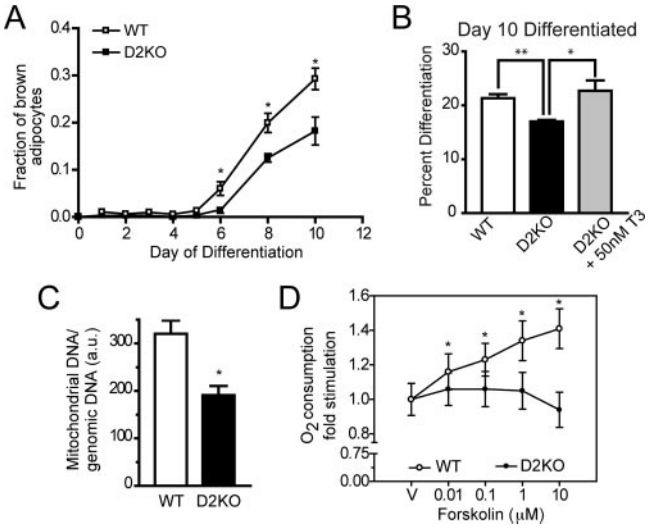

FIG. 3. Impaired D2KO brown adipocyte differentiation. A, Brown preadipocytes were isolated from iBAT of WT and D2KO mice and differentiated in culture. Percentage of differentiated brown adipocytes determined by immunocytochemistry after staining with BODIPY 493/503. B, Treatment of D2KO preadipocytes cultures with 50 nM T3 during the early stages of differentiation (d 0–4) restores the WT percentage differentiation at d 10. C, Mitochondrial content in WT and D2KO d 10 brown adipocytes by quantification of Cox1/2 and Cox8 gDNA by qRT-PCR, expressed as mitochondrial/genomic DNA ratio. D, O_2 consumption of WT and D2KO d 10 brown adipocyte cultures in response to increasing concentrations of forskolin. A–D, Values are mean ± SEM of 3–30 data points unless otherwise indicated. *, $P < 0.05$; and **, $P < 0.01$ *vs.* WT (or as indicated) by Student's *t* test.

D2KO cells terminally differentiate into brown adipocytes at each time-point analyzed (Fig. 3A). This was verified by flow cytometry (Supplemental Fig. 3A) and oil-red-O staining intensity (Supplemental Fig. 3B). Notably, these changes are connected with a decrease in thyroid hormone signaling, given the complete rescue of the D2KO phenotype by treatment with 50 nM T3 (Fig. 3B). If not rescued, the D2KO brown adipocytes have approximately 40% fewer mitochondria (Fig. 3C) and impaired cAMP-induced oxidative capacity (Fig. 3D). Using a XF24 instrument that monitors oxygen (O_2) consumption, D2KO brown adipocyte cultures failed to increase O_2 consumption in a wide range of forskolin concentrations (Fig. 3D). Collectively, these findings indicate a defect in differentiation that results in a substantial impairment in the mature adipocyte function, such as lipid accumulation and oxidative capacity.

D2KO BAT has decreased antioxidant defenses and is susceptible to oxidative stress

As an unbiased approach to elucidate additional transcriptional pathways that underlie the D2KO BAT phenotype, we used microarray analysis of E18.5 BAT from WT and D2KO littermates. This approach confirmed our previous observations (Fig. 2 and data not shown) and led to additional genes with reported roles in regulation of ROS formation and damage, including *GPx3*, *Mb*, *Msrb2*, and *PKD1*. The expression of these genes (with the exception of *PKD1*) was greatly increased throughout the course of BAT development (Fig. 4A). Glutathione peroxidase 3 (*GPx3*), which is an antioxidant that is highly expressed in BAT (20), was significantly less (38%) in BAT pads of D2KO mice. Also, reductions of approximately 30% were seen in expression of methionine sulfoxide reductase B2 (*MsrB2*), an enzyme that repairs oxidized proteins and protects against oxidative stress (21), and protein kinase D1 (*PKD1*), which regulates protective signaling in response to ROS (22). Most dramatically, expression of myoglobin (*Mb*) was reduced by 72% in E18.5 D2KO BAT compared with WT. Mb, which is known to increase in BAT during cold exposure (23), plays roles in oxygen transport and scavenging of ROS (24). Importantly, this decrease in ROS defense coincided with oxidative damage, as evidenced by increased lipid peroxidation end products (as observed by immunoblotting for malondialdehyde) in E18.5 D2KO BAT (Fig. 4B). These data indicate that the absence of D2 modifies the developing BAT transcriptome, limiting defenses against ROS accumulation and oxidative stress.

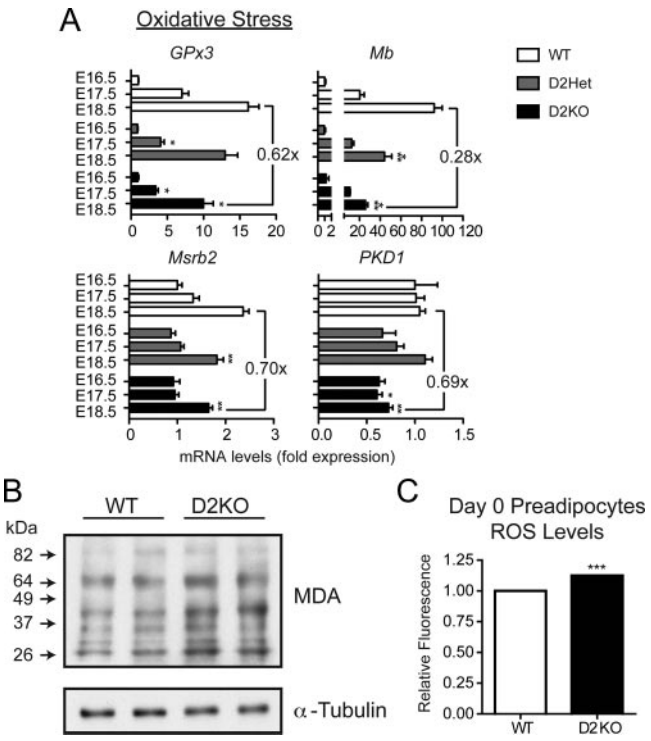

FIG. 4. Oxidative stress in D2KO embryonic BAT. A, Expression of genes related to oxidative stress response processes in iBAT from WT, D2Het, and D2KO embryos at embryonic d E16.5, E17.5, and E18.5. mRNA levels determined by qRT-PCR are graphed relative to E16.5 WT expression. *, $P < 0.05$; **, $P < 0.01$; and ***, $P < 0.001$ *vs.* WT of respective day by one-way ANOVA with Dunnet's Multiple correction. B, Lipid peroxidation in iBAT lysates from E18.5 WT and D2KO littermates as indicated by immunoblotting for malonaldehyde (MDA). α-Tubulin shown as loading control. C, Average CM-H_2DCFDA fluorescence in d 0 brown preadipocytes after quantification with flow cytometry. ***, $P < 0.001$ by Student's *t* test.

To confirm that these changes in gene expression were leading to accumulation of ROS, we incubated *in vitro* differentiated D2KO brown adipocytes with the ROS sensitive dye CM-H_2DCFDA to quantify signal intensity. Indeed, d 10 D2KO brown adipocytes exhibited higher levels of ROS (Supplemental Fig. 4). Elevated ROS levels were observed even in D2KO preadipocytes at d 0, a time at which differences based solely on decreased fat cell number could be avoided. Notably, ROS levels in D2KO preadipocytes are already 12.5% higher than WT, suggesting that defects in gene expression are present at early stages of differentiation (Fig. 4C). In fact, microarray analysis of these preadipocytes identified decreases in genes involved in ROS metabolic processes (Supplemental Table 2), which was determined by GeneMAPP2 evaluation to be one of the most significantly altered biological pathways in D2KO brown preadipocytes (Z scores >10, $P < 0.05$; Supplemental Table 2). Collectively, these patterns of altered gene expression indicate that D2KO preadipocytes are at higher risk of developing oxidative stress due to ROS accumulation.

Next, we looked for potential metabolic perturbations downstream of oxidative stress. Specifically, we examined insulin signaling via the PI3K/Akt pathway in D2KO brown preadipocytes, because oxidative stress has been reported to trigger insulin resistance in adipocytes (25). Remarkably, insulin signaling, as determined by an active phosphorylated form of Akt (Ser473), was much lower in D2KO preadipocytes, when exposed to varying levels of insulin (Fig. 5, A and B). A link between D2 activity and insulin signaling was confirmed by chemically inactivating D2 with rT3 in WT preadipocytes, which produced similar defects in Akt phosphorylation (Fig. 5, C and D). Oxidative stress can induce insulin resistance through inhibitory phosphorylation of IRS1 by IKK (26, 27). Thus, increased IRS1 Ser307 phosphorylation in D2KO preadipocytes (Fig. 5E) without changing expression of key insulin signaling components (Supplemental Fig. 5, A and B) suggests that oxidative stress leads to the decreased insulin signaling. This is corroborated by increased IκBα phosphorylation (Fig. 5F), which is a downstream effector of IKK and consistent with NFκB activation upon cellular stress. Finally, we treated WT and D2KO cells with the anti-oxidant ascorbic acid, which rescued insulin signaling in the D2KO to WT levels, indicating that elevated levels of ROS lead to decreased insulin signaling in these cells (Fig. 5, G and H).

Supplemental insulin (3 nM) is the predominant force driving adipogenesis in our *in vitro* model, so we hypothesized that the defective differentiation phenotype that is observed in the D2KO cells could be due to disruption of insulin signaling. In fact, this is confirmed by experiments in which differentiation was carried out in the absence of supplemental insulin, but rather with an adipogenic cocktail (IBMX, dexamethasone, and indomethacin) for two d. In this setting, differences in the relative number of mature brown adipocytes between WT and D2KO cells were dissipated (Fig. 5I). These findings suggest that other stimuli present during BAT development may bypass a more severe defect in brown adipogenesis, such as the differentiation phenomenon that is observed when insulin alone is pushing the conversion of preadipocytes to brown adipocytes.

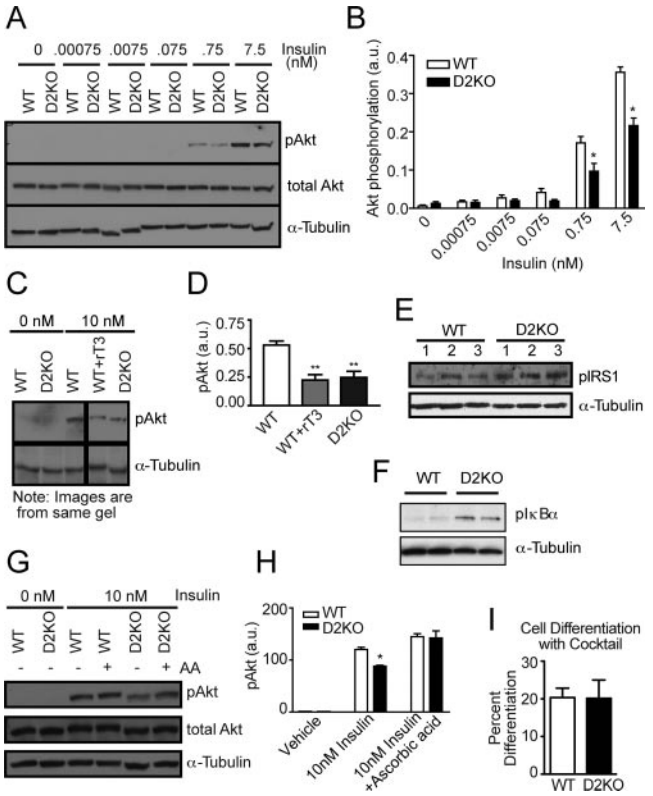

FIG. 5. ROS causes decreased insulin signaling. A and B, WT and D2KO d 0 brown preadipocytes were serum starved for 20 h, treated for 5 min with varying doses of insulin, and levels of pAkt (Ser473), total Akt, and α-tubulin determined by immunoblotting. C and D, Immunoblotting of pAkt (S473) and α-tubulin in vehicle-treated WT and D2KO preadipocytes, as well as WT preadipocytes treated with rT3 since differentiation. Images are from different regions of same gel. E, Immunoblot analysis of d 0 serum starved WT and D2KO brown preadipocytes for phospho-IRS1 (S307) and α-tubulin. F, Immunoblot of phosphorylated IκBα in extracts from d 2 WT and D2KO brown preadipocytes. G and H, Treatment with the antioxidant ascorbic acid restores phosporylation of pAkt (S473) in D2KO brown preadipocytes to WT levels. I, Analysis of WT and D2KO preadipocytes differentiated with adipogenic cocktail, as described in text. Fractional number of brown adipocytes quantified by immunocytochemistry as previously described. Values are mean ± SEM of 2–4 data points. B, D, and H, Quantification of Akt (Ser473) phosphorylation by normalization to α-tubulin levels and total signal on each Western blot. Values are mean ± SEM of 3–5 data points. *, $P < 0.05$ by Student's *t* test (B and H). **, $P < 0.01$ by one way ANOVA with Newman-Keuls Multiple Comparison (D).

Discussion

The present study demonstrates that impaired BAT thermogenesis in the D2KO mouse stems from an embryologic defect due to a role played by D2-generated T3 in enhancing the expression of BAT-selective genes. Notably, these changes in gene expression are observed *in utero*, without a thermogenic challenge, which highlights the relevance of D2 and its ability to amplify thyroid hormone signaling in a developmental setting. As BAT develops, coordinated changes in deiodinase expression (*Dio2* induction and *Dio3* suppression) enhance thyroid hormone signaling (Fig. 1, C–F), which can be linked to peak T3 concentration in developing BAT (28). A similar mechanism has been shown in other developing tissues, including the coordinated expression of D2 and D3 at a critical period of cochlear development in mammals, where absence of either deiodinase leads to inappropriate exposure to T3 and results in deafness (10, 29, 30). Our data indicate that this deiodinase-based mechanism plays a hitherto under-appreciated role in the developing BAT.

The process of brown adipocyte differentiation involves molecular pathways that are common to both white and brown adipocyte lineages and pathways that are BAT-specific, including transcriptional changes that confer its thermogenic function (31). It is well established that thyroid hormone plays a role in adipogenesis *per se*. T3 is frequently used in adipogenic cocktails and is absolutely required for terminal differentiation, possibly through regulation of PPARγ (32, 33). What is remarkable and evidenced by our data are that the deiodinases, by increasing thyroid hormone signaling, can affect BAT development without changing the extracellular levels of thyroid hormone. The inactivation of a single component of this mechanism (*i.e.* D2), results in embryonic BAT with decreased expression of key thermogenic genes, without gross impairments in the adipogenic process (Fig. 2, B–D). Only with *in vitro* differentiated D2KO brown preadipocytes do we find defective differentiation, suggesting the existence of potent *in vivo* compensatory mechanisms. The key aspect here is that D2 is necessary for coordinating the expression of genes that contribute to the identity of BAT *in vivo*, and, thus, plays a role in its thermogenic capacity. In fact, when fetal D2 activity is blocked by iopanoic acid treatment of pregnant mothers, newborn rats show a blunted response to thermal stress upon birth (13).

Given that T3-TR modifies gene expression, we show that brown preadipocytes exposed to T3 have increased expression of *UCP1*, *Dio2*, and *PGC-1α*, transcripts found to be decreased in D2KO embryonic BAT (Fig. 2, D and E). In a variety of settings, *UCP1*, *Dio2*, and *PGC-1α* have been shown to be T3-responsive genes (2, 11, 34, 35)

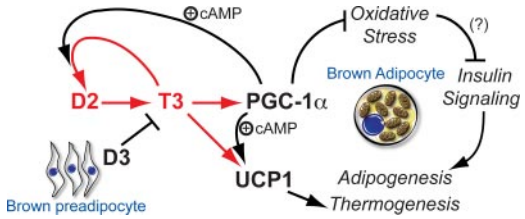

FIG. 6. Proposed model of positive feedback involving *Dio2*, *PGC-1α*, and *UCP1* expression during BAT development. Schematic representation of the proposed role of D2 and D2-generated T3 in the development of brown adipocytes. D3, which decreases thyroid hormone signaling, is highest in the undeveloped brown preadipocyte. As the brown preadipocyte matures, D2, by enhancing thyroid hormone signaling, increases expression of *PGC-1α*, which coactivates TR, leading to enhanced *UCP1* expression. Notably, *Dio2* is also upregulated by increased T3-signaling. These changes provide the mature brown adipocyte with its thermogenic function and also limit oxidative stress. If oxidative stress goes unchecked, then insulin signaling and adipogenesis may be altered.

and have been independently linked to BAT function. Additionally, PGC-1α is a partner of PPARγ and TRβ in coactivating the *UCP1* promoter (36) and is necessary for the increased expression of *UCP1* and *Dio2* after stimulation with a cyclic AMP agonist (37). The novelty of our findings is that the expression of these three genes is interconnected during BAT development, with D2 generating T3 that will further enhance its own production and induce PGC-1α and UCP1 in a positive feedback loop (Fig. 6). Notably, brown adipocytes deficient in PGC-1α exhibit a relatively normal transcriptome with defects lying primarily in thermogenic activation by cAMP (37). This is a milder phenotype than that of D2KO cells, emphasizing a predominant role for D2 in BAT development.

Embryonic BAT lacking D2-generated T3 is more susceptible to oxidative damage, which results from uncontrolled oxidative stress by a decrease in anti-ROS defenses (Fig. 4, A and B). However, acute T3-responsiveness was not found in the subset of ROS-detoxifying genes perturbed in the D2KO BAT (data not shown). PGC-1α has been shown to be a critical regulator of ROS detoxification through induction of ROS-scavenging enzymes (38). Thus, D2 could play a role upstream of PGC-1α, where D2 generating T3 induces PGC-1α, turning on an anti-ROS gene program. While it is not possible yet to conclude whether oxidative damage in D2KO E18.5 BAT contributes toward decreased insulin signaling *in vivo*, our *in vitro* D2KO brown preadipocyte data strongly suggest that under the appropriate conditions ROS leads to decreased insulin signaling and impaired differentiation. It is interesting to speculate that such mechanisms could also play a role in other settings in which *Dio2* and *PGC-1α* are highly expressed, such as the brain.

Our analysis of the mechanisms underlying impaired thermogenic function of D2KO BAT has led us to the identification of a critical deiodinase-mediated pathway in

BAT development. This explains the hypothermic and obesity phenotype observed in adult D2KO mice. It is clear that D2 acts on an important aspect of brown adipocyte biology (*i.e.* BAT identity), but other pathways might also be involved (*i.e.* protection from oxidative damage). Here we identified a developmental relationship between D2-generated T3, UCP1, and PGC-1α in the absence of a thermogenic stimulus (Fig. 6). Uncovering this connection illustrates how such a pathway is critical for maintenance of energy homeostasis in adulthood.

Acknowledgments

We are grateful for the technical assistance of Matthew Rosene and Kevin Johnson (Diabetes Research Institute Immunohistochemistry Core).

Address all correspondence and requests for reprints to: Antonio C. Bianco, M.D., Ph.D., University of Miami Miller School of Medicine, 1400 Northwest 10th Street, Dominion Towers Suite 816, Miami, Florida 33136. E-mail: abianco@deiodinase.org.

This work was supported in part by National Institutes of Health Grant DK65055 and by Dana-Farber Microarray Core Facility.

Present address for S.R.: 200 Technology Square, Suite 300, Cambridge, Massacusetts 02138. Current address for M.A.C.: Centro de Ciências Naturais e Humanas, Universidade Federal do ABC, Santo André, Sao Paulo, Brazil.

Disclosure Summary: The authors have nothing to declare.

References

1. **Nedergaard J, Cannon B** 2010 The changed metabolic world with human brown adipose tissue: therapeutic visions. Cell Metab 11: 268–272
2. **Bianco AC, Sheng XY, Silva JE** 1988 Triiodothyronine amplifies norepinephrine stimulation of uncoupling protein gene transcription by a mechanism not requiring protein synthesis. J Biol Chem 263:18168–18175
3. **Sellers EA, You SS** 1950 Role of the thyroid in metabolic responses to a cold environment. Am J Physiol 163:81–91
4. **Bianco AC, Silva JE** 1987 Intracellular conversion of thyroxine to triiodothyronine is required for the optimal thermogenic function of brown adipose tissue. J Clin Invest 79:295–300
5. **Gereben B, Zavacki AM, Ribich S, Kim BW, Huang SA, Simonides WS, Zeöld A, Bianco AC** 2008 Cellular and molecular basis of deiodinase-regulated thyroid hormone signaling. Endocr Rev 29:898–938
6. **Simonides WS, Mulcahey MA, Redout EM, Muller A, Zuidwijk MJ, Visser TJ, Wassen FW, Crescenzi A, da-Silva WS, Harney J, Engel FB, Obregon MJ, Larsen PR, Bianco AC, Huang SA** 2008 Hypoxia-inducible factor induces local thyroid hormone inactivation during hypoxic-ischemic disease in rats. J Clin Invest 118:975–983
7. **Schneider MJ, Fiering SN, Pallud SE, Parlow AF, St Germain DL, Galton VA** 2001 Targeted disruption of the type 2 selenodeiodinase gene (DIO2) results in a phenotype of pituitary resistance to T4. Mol Endocrinol 15:2137–2148
8. **de Jesus LA, Carvalho SD, Ribeiro MO, Schneider M, Kim SW, Harney JW, Larsen PR, Bianco AC** 2001 The type 2 iodothyronine deiodinase is essential for adaptive thermogenesis in brown adipose tissue. J Clin Invest 108:1379–1385
9. **Christoffolete MA, Linardi CC, de Jesus L, Ebina KN, Carvalho SD, Ribeiro MO, Rabelo R, Curcio C, Martins L, Kimura ET, Bianco AC** 2004 Mice with targeted disruption of the Dio2 gene have cold-induced overexpression of the uncoupling protein 1 gene but fail to increase brown adipose tissue lipogenesis and adaptive thermogenesis. Diabetes 53:577–584
10. **Ng L, Hernandez A, He W, Ren T, Srinivas M, Ma M, Galton VA, St Germain DL, Forrest D** 2009 A protective role for type 3 deiodinase, a thyroid hormone-inactivating enzyme, in cochlear development and auditory function. Endocrinology 150:1952–1960
11. **Martinez-deMena R, Hernández A, Obregón MJ** 2002 Triiodothyronine is required for the stimulation of type II 5′-deiodinase mRNA in rat brown adipocytes. Am J Physiol Endocrinol Metab 282: E1119–E1127
12. **Watanabe M, Houten SM, Mataki C, Christoffolete MA, Kim BW, Sato H, Messaddeq N, Harney JW, Ezaki O, Kodama T, Schoonjans K, Bianco AC, Auwerx J** 2006 Bile acids induce energy expenditure by promoting intracellular thyroid hormone activation. Nature 439: 484–489
13. **Giralt M, Martin I, Iglesias R, Viñas O, Villarroya F, Mampel T** 1990 Ontogeny and perinatal modulation of gene expression in rat brown adipose tissue. Unaltered iodothyronine 5′-deiodinase activity is necessary for the response to environmental temperature at birth. Eur J Biochem 193:297–302
14. **Smas CM, Sul HS** 1993 Pref-1, a protein containing EGF-like repeats, inhibits adipocyte differentiation. Cell 73:725–734
15. **Lin SP, Youngson N, Takada S, Seitz H, Reik W, Paulsen M, Cavaille J, Ferguson-Smith AC** 2003 Asymmetric regulation of imprinting on the maternal and paternal chromosomes at the Dlk1-Gtl2 imprinted cluster on mouse chromosome 12. Nat Genet 35: 97–102
16. **Hernandez A, Garcia B, Obregon MJ** 2007 Gene expression from the imprinted Dio3 locus is associated with cell proliferation of cultured brown adipocytes. Endocrinology 148:3968–3976
17. **Farmer SR** 2006 Transcriptional control of adipocyte formation. Cell Metab 4:263–273
18. **Zhou Z, Yon Toh S, Chen Z, Guo K, Ng CP, Ponniah S, Lin SC, Hong W, Li P** 2003 Cidea-deficient mice have lean phenotype and are resistant to obesity. Nat Genet 35:49–56
19. **Samuels HH, Tsai JS** 1973 Thyroid hormone action in cell culture: domonstration of nuclear receptors in intact cells and isolated nuclei. Proc Natl Acad Sci USA 70:3488–3492
20. **Lee YS, Kim AY, Choi JW, Kim M, Yasue S, Son HJ, Masuzaki H, Park KS, Kim JB** 2008 Dysregulation of adipose glutathione peroxidase 3 in obesity contributes to local and systemic oxidative stress. Mol Endocrinol 22:2176–2189
21. **Cabreiro F, Picot CR, Perichon M, Castel J, Friguet B, Petropoulos I** 2008 Overexpression of mitochondrial methionine sulfoxide reductase B2 protects leukemia cells from oxidative stress-induced cell death and protein damage. J Biol Chem 283:16673–16681
22. **Storz P** 2007 Mitochondrial ROS–radical detoxification, mediated by protein kinase D. Trends Cell Biol 17:13–18
23. **Watanabe M, Yamamoto T, Kakuhata R, Okada N, Kajimoto K, Yamazaki N, Kataoka M, Baba Y, Tamaki T, Shinohara Y** 2008 Synchronized changes in transcript levels of genes activating cold exposure-induced thermogenesis in brown adipose tissue of experimental animals. Biochim Biophys Acta 1777:104–112
24. **Ordway GA, Garry DJ** 2004 Myoglobin: an essential hemoprotein in striated muscle. J Exp Biol 207:3441–3446
25. **Houstis N, Rosen ED, Lander ES** 2006 Reactive oxygen species have a causal role in multiple forms of insulin resistance. Nature 440:944–948
26. **Bloch-Damti A, Potashnik R, Gual P, Le Marchand-Brustel Y, Tanti JF, Rudich A, Bashan N** 2006 Differential effects of IRS1 phosphorylated on Ser307 or Ser632 in the induction of insulin resistance by oxidative stress. Diabetologia 49:2463–2473

27. **Gao Z, Hwang D, Bataille F, Lefevre M, York D, Quon MJ, Ye J** 2002 Serine phosphorylation of insulin receptor substrate 1 by inhibitor κ B kinase complex. J Biol Chem 277:48115–48121
28. **Carmona MC, Iglesias R, Obregón MJ, Darlington GJ, Villarroya F, Giralt M** 2002 Mitochondrial biogenesis and thyroid status maturation in brown fat require CCAAT/enhancer-binding protein α. J Biol Chem 277:21489–21498
29. **Campos-Barros A, Amma LL, Faris JS, Shailam R, Kelley MW, Forrest D** 2000 Type 2 iodothyronine deiodinase expression in the cochlea before the onset of hearing. Proc Natl Acad Sci USA 97: 1287–1292
30. **Ng L, Goodyear RJ, Woods CA, Schneider MJ, Diamond E, Richardson GP, Kelley MW, Germain DL, Galton VA, Forrest D** 2004 Hearing loss and retarded cochlear development in mice lacking type 2 iodothyronine deiodinase. Proc Natl Acad Sci USA 101: 3474–3479
31. **Kajimura S, Seale P, Spiegelman BM** 2010 Transcriptional control of brown fat development. Cell Metab 11:257–262
32. **Ying H, Araki O, Furuya F, Kato Y, Cheng SY** 2007 Impaired adipogenesis caused by a mutated thyroid hormone α1 receptor. Mol Cell Biol 27:2359–2371
33. **Ailhaud G, Dani C, Amri EZ, Djian P, Vannier C, Doglio A, Forest C, Gaillard D, Négrel R, Grimaldi P** 1989 Coupling growth arrest and adipocyte differentiation. Environ Health Perspect 80:17–23
34. **Irrcher I, Adhihetty PJ, Sheehan T, Joseph AM, Hood DA** 2003 PPARγ coactivator-1α expression during thyroid hormone- and contractile activity-induced mitochondrial adaptations. Am J Physiol Cell Physiol 284:C1669–C1677
35. **Weitzel JM, Radtke C, Seitz HJ** 2001 Two thyroid hormone-mediated gene expression patterns in vivo identified by cDNA expression arrays in rat. Nucleic Acids Res 29:5148–5155
36. **Puigserver P, Wu Z, Park CW, Graves R, Wright M, Spiegelman BM** 1998 A cold-inducible coactivator of nuclear receptors linked to adaptive thermogenesis. Cell 92:829–839
37. **Uldry M, Yang W, St-Pierre J, Lin J, Seale P, Spiegelman BM** 2006 Complementary action of the PGC-1 coactivators in mitochondrial biogenesis and brown fat differentiation. Cell Metab 3:333–341
38. **St-Pierre J, Drori S, Uldry M, Silvaggi JM, Rhee J, Jäger S, Handschin C, Zheng K, Lin J, Yang W, Simon DK, Bachoo R, Spiegelman BM** 2006 Suppression of reactive oxygen species and neurodegeneration by the PGC-1 transcriptional coactivators. Cell 127:397–408